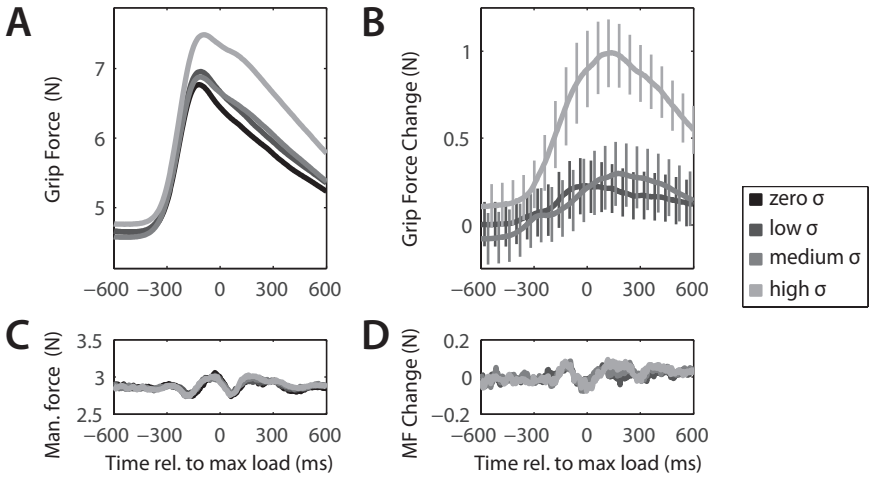

Figure S1. Grip and manipulatory force profiles for different variability levels in Experiment 1b.
Same as panels DEGH of Figure 2, but for Experiment 1b, illustrating the same pattern of increases in the average GF profiles with increased variability. Note that in Experiment 1b the low, medium and high variability levels have ~33% lower values for σ compared to the corresponding levels in Experiment 1 (1.2, 2.4 and 3.6 Ns/m for Experiment 1b vs 1.8, 3.6 and 5.4 Ns/m for the low, medium and high σ blocks in Experiment 1).

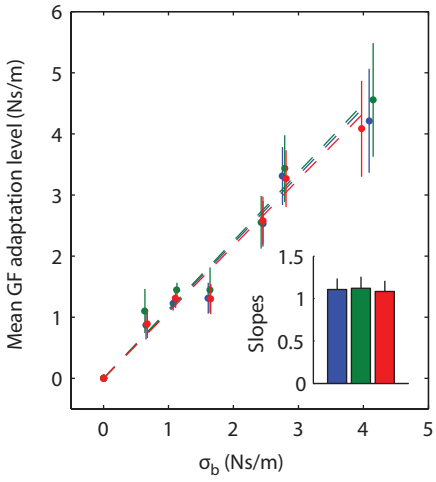

Figure S2. Choice of window size has little effect on the estimation of GF sensitivity.
Data combined across Experiments 1 and 1b.
Main panel: Plot of mean GF adaptation level for each value of σ (analogous to Figure 2I). Blue indicates the results observed when excluding the first 15 trials of each block. This is the same window used for analysis in the main text (trials 16:40 and 45:50 for Experiment 1; trials 16:40, 45:90 and 95:100 for Experiment 1b). Red indicates results using a smaller, 25-trial window matched across experiments that avoids all trials immediately following a break (red, trials 16:40 for both Experiments 1 and 1b). Cyan indicates results using all available trials for each block (trials 1:50 for Experiment 1; trials 1:100 for Experiment 1b).
Inset: Slopes (sensitivity estimates) of the relationships plotted in the main panel, indicating similar results across different window sizes.

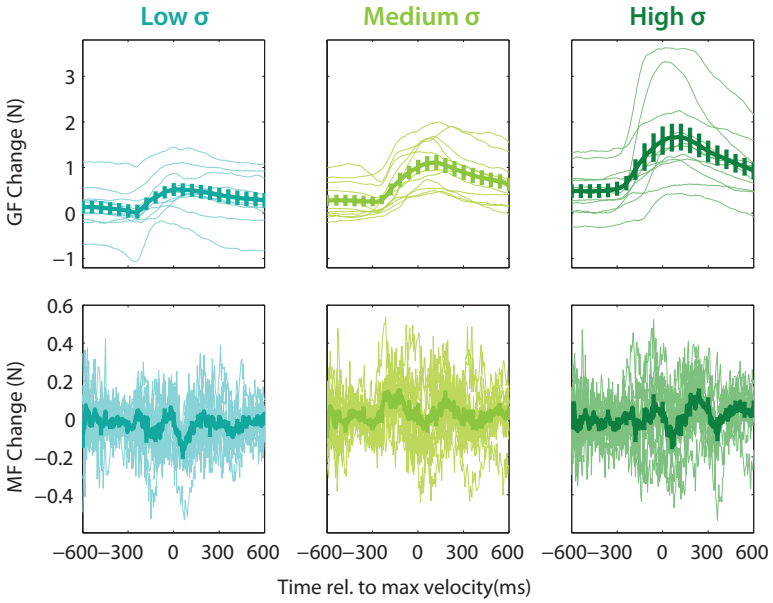

Figure S3. Grip force (top row) and manipulatory force (bottom row) changes with respect to the zero-variability block in Experiment 1 (Compare to Figure 2EH). Shown are both individual subject data (thin lines) and mean±SEM across subjects (thick lines with errorbars), illustrating the increases in GF (but not MF) with increasing variability.

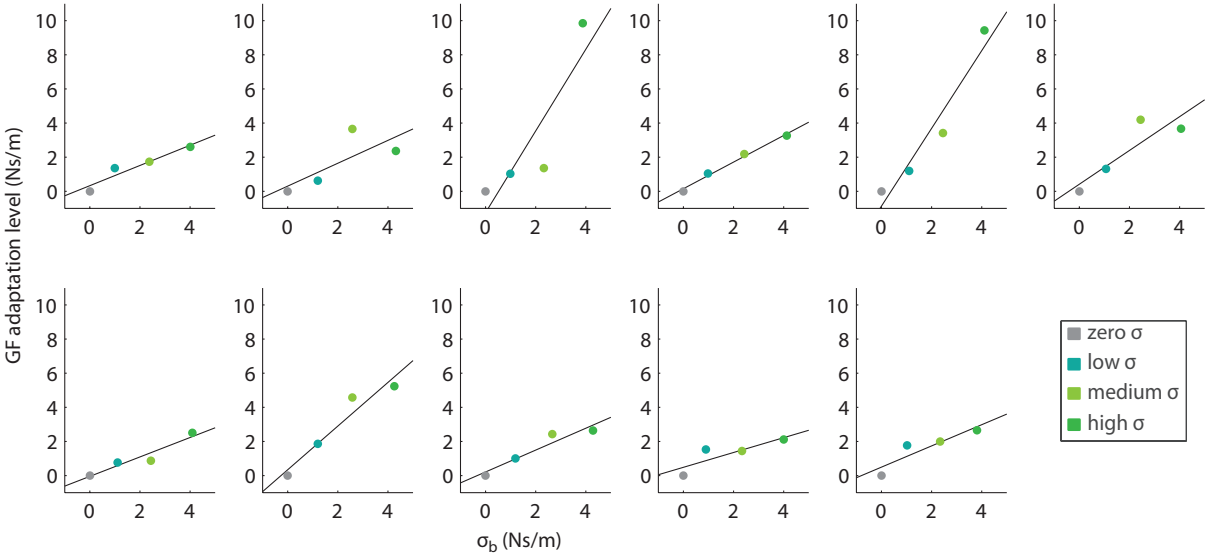

Figure S4. The upregulation of grip force levels with standard deviation is apparent in all 11 subjects in Experiment 1. Each panel shows grip force data from an individual subject, with each point representing one block type. Black lines show linear fits.

Grip forces during error-clamp (EC) and non-EC trials

In our experiments, GF profiles were measured in all trials, whereas MF profiled were measured during EC trials only. This is the case because, MF profile measurements can be dramatically distorted if EC trials are not used (Sing et al., 2009). However, these distortions should not affect GF profile measurements. An analysis of the GF profiles for EC and non-EC trials shows similar results (see Figure S3), albeit with cleaner findings for the non-EC trials, which is to be expected because of a 4-fold greater amount of data is available for these trials. Thus, we found no reason to dismiss 4/5 of the GF data and we included both EC and non-EC trials in our analyses.

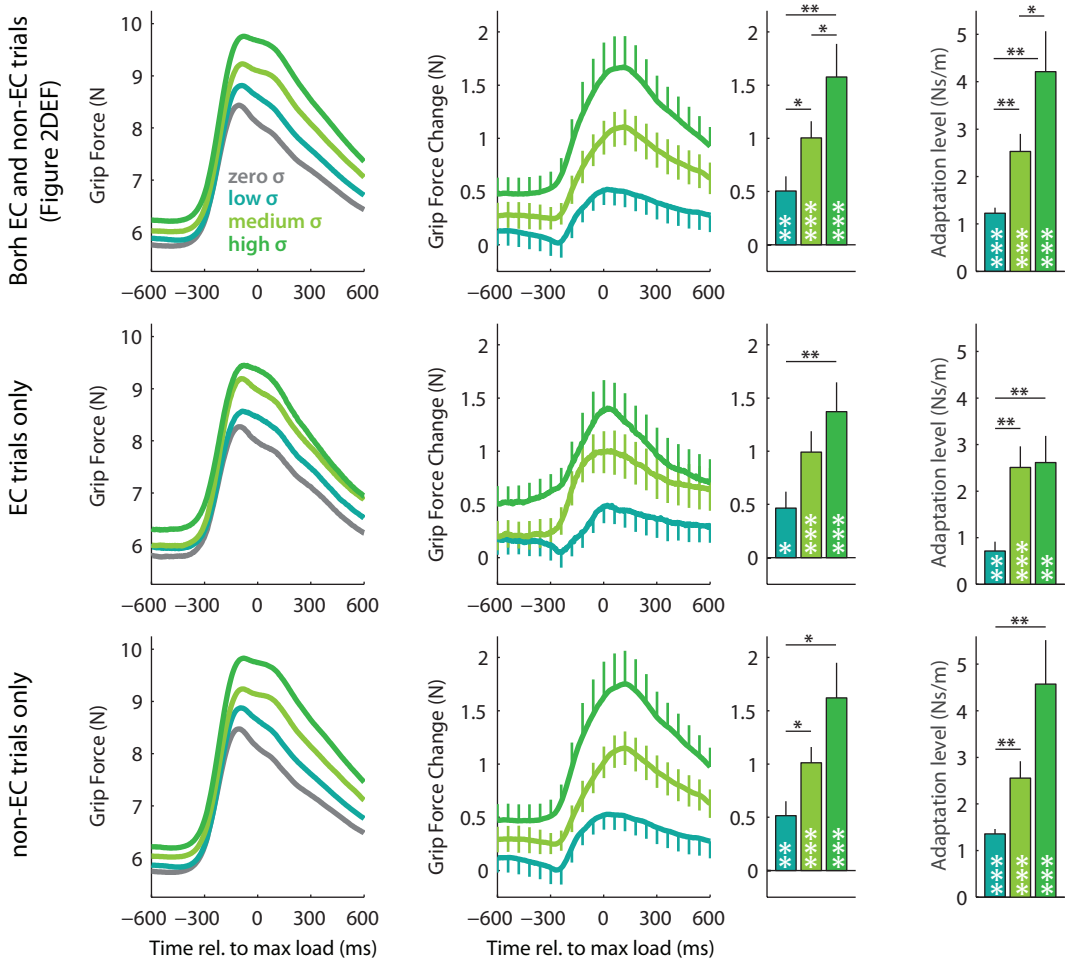

Figure S5. The results of Experiment 1 are similar for error-clamp trials vs. non-error-clamp trials. The format of each row is the same as Figure 2D-F in the manuscript. Top row: analysis using both trial types (row is the same as Figure 2D-F). Middle row: same analysis but for error-clamp trials only. Bottom row: same analysis for non-error-clamp trials only.

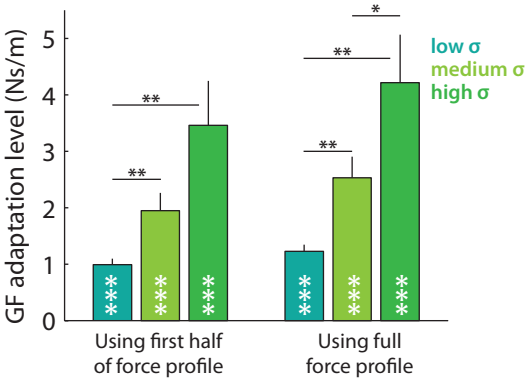

Figure S6. The scaling of GF levels with variability is not due to asymmetries in GF profiles between the first and second half of the movement. Grip force adaptation coefficients for the different variability levels in Experiment 1 calculated based on either the first part of the movement (up to the point of maximum velocity, left) or based on the full movement (i.e. as in the main analysis of our paper, right and Figure 2). Under both methods, GF levels scale with the variability level. There is a slight but consistent reduction in these estimates when only the first part of the movement is used. * p<0.05, ** p<0.01, *** p<0.001 (single-tailed paired t-tests).

Analysis of carryover effects

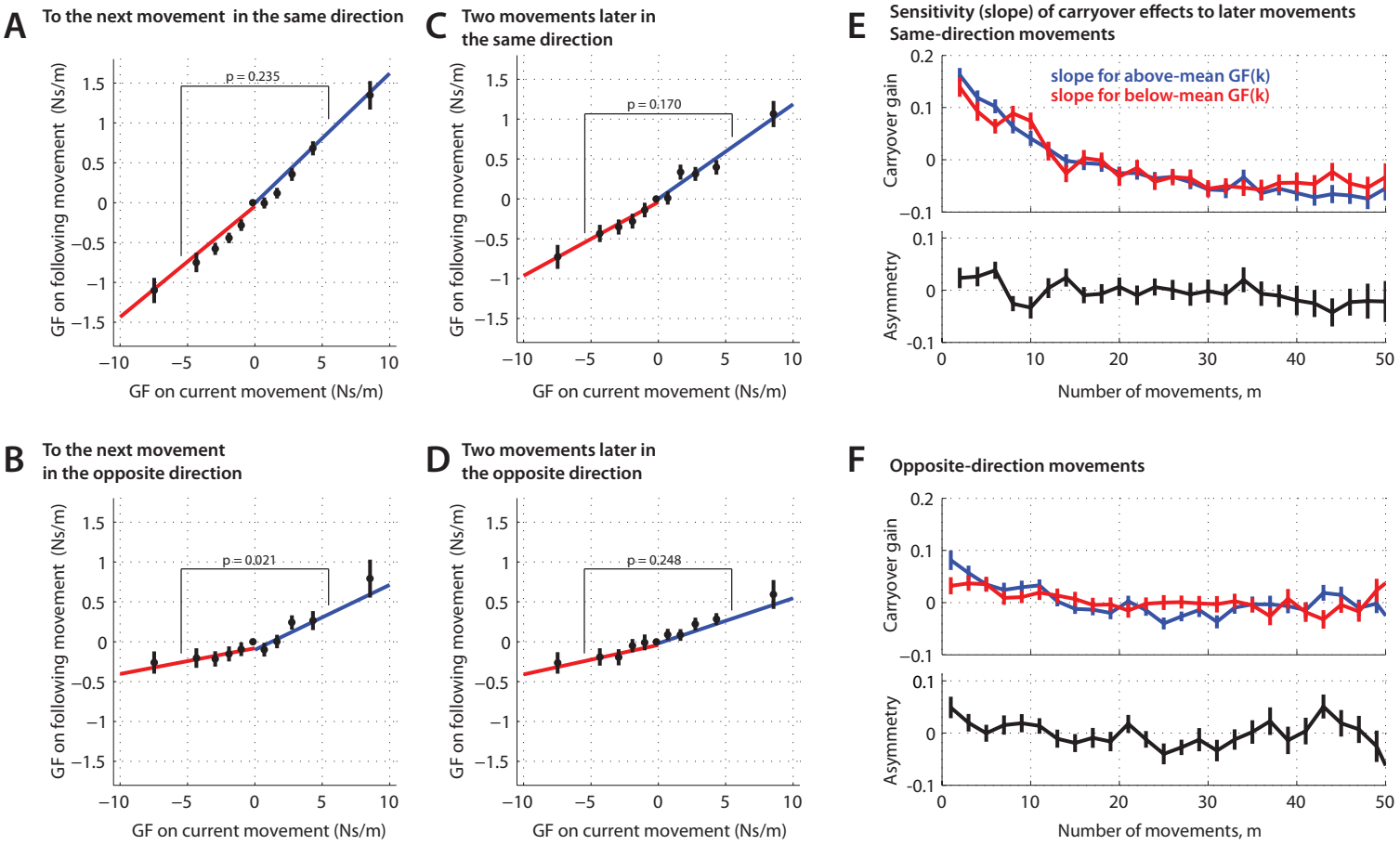

Figure R7: Trial-to-trial GF carryover effects in our data are small and largely symmetric.
A: Carryover effects in Experiments 1a, 1b, and 1c. The x-axis shows the (mean-referenced) GF on a given current movement, split into 11 quantiles, whereas the y-axis shows the amount of carryover to the next movement in the same movement direction. The y-axis is also referenced to the center quantile. To assess any asymmetry between carryover effects for above- vs. below-mean current GF, we performed separate linear fits (blue vs. red, respectively) which showed similar slopes.
B: Same as A but for the next movement that is in the opposite direction.
C, D: Same as A or B but for carryover to two movements later in the same and opposite direction, respectively.
E: Slopes (sensitivities) for the carryover of above-mean (blue) vs. below-mean (red) GFs m movements later. Shown are movements that are on the same direction as the current movement. Carryover effects last for about 5-10 trials and are largely symmetric for above- vs. below-mean GFs, as illustrated in the lower panel which shows the asymmetry between these carry-over effects (as the difference in carryover gains). Note that this asymmetry is small and not consistently positive.
F: Same as C but for trials on the opposite direction as the current trial. Carryover effects are weaker compared to C and also appear to only last for about 5-10 trials.

Investigating the effects of trial-to-trial GF carryover in the sensitivity of GFs to changes in environmental variability

To systematically investigate the potential effect of asymmetric trial-to-trial GF carryover on the data, we modeled trial-to-trial GF responses, $x(k)$, as the sum of a normally-varying process, $u(k)$, and carryover effects driven by carryover gains c_p and c_n for above-mean (>0) and below-mean (<0) x:

$$x(k) = u(k) + \sum_{i=1}^{N} c_{p,i} x_p(k-i) + \sum_{i=1}^{N} c_{n,i} x_n(k-i) \quad (1)$$

Where

$$x_p(k) = \begin{cases} x(k), & x(k) > 0 \\ 0, & x(k) < 0 \end{cases} \qquad x_n(k) = \begin{cases} 0, & x(k) > 0 \\ x(k), & x(k) < 0 \end{cases}$$

Thus, the expected value of $x(k)$ should equal

$$E(x(k)) = E(u(k)) + \sum_{i=1}^{N} c_{p,i} E\left(x_p(k-i)\right) + \sum_{i=1}^{N} c_{n,i} E(x_n(k-i))$$

$$\Longrightarrow E(x(k)) = 0 + E\left(x_p(k)\right) \sum_{i=1}^{N} c_{p,i} + E\left(x_n(k)\right) \sum_{i=1}^{N} c_{n,i}$$

For easier notation, we will use

$$E\left(x(k)\right) = \mu, \qquad E\left(x_p(k)\right) = \mu_p, \qquad E\left(x_n(k)\right) = \mu_n, \qquad \sum_{i=1}^{N} c_{p,i} = C_p\,, \qquad \sum_{i=1}^{N} c_{n,i} = C_n$$

$$\Longrightarrow \mu = \mu_p C_p + \mu_n C_n \quad (2)$$

Assuming that the output $x(k)$ is normally distributed with a standard deviation of σ, we can express μ_p and μ_n as functions of μ:

$$\mu_p = \int_0^{\infty} x \frac{1}{\sqrt{2\pi}\sigma} e^{-\frac{(x-\mu)^2}{2\sigma^2}} dx = \cdots = \frac{\sigma e^{-\frac{\mu^2}{2\sigma^2}}}{\sqrt{2\pi}} + \frac{\mu}{2}\left(1 - \operatorname{erf}\left(-\frac{\mu}{\sigma\sqrt{2}}\right)\right) \quad (3a)$$

In an analogous fashion,

$$\mu_n = \frac{\sigma e^{-\frac{\mu^2}{2\sigma^2}}}{\sqrt{2\pi}} + \frac{\mu}{2}\left(1 + \operatorname{erf}\left(-\frac{\mu}{\sigma\sqrt{2}}\right)\right) \quad (3b)$$

We can thus get μ by combining Equations (2) and (3):

$$\mu = \frac{\sigma e^{-\frac{\mu^2}{2\sigma^2}}}{\sqrt{2\pi}} - \frac{\mu}{2}\left(1 + \operatorname{erf}\left(-\frac{\mu}{\sigma\sqrt{2}}\right)\right)\left(C_p - C_n\right) + \mu C_p \quad (4)$$

While equation (4) does not offer an explicit expression for μ, it does define a specific relationship between μ and σ. Note that dividing both sides of (4) by σ yields a relationship that only depends on the ratio μ/σ:

$$\frac{\mu}{\sigma} = \frac{e^{-\frac{1}{2}\left(\frac{\mu}{\sigma}\right)^2}}{\sqrt{2\pi}} - \frac{1}{2}\frac{\mu}{\sigma}\left(1 + \mathrm{erf}\left(-\frac{1}{\sqrt{2}}\frac{\mu}{\sigma}\right)\right)\left(C_p - C_n\right) + \frac{\mu}{\sigma}C_p \quad (5)$$

Thus, solving Equation (5) for μ/σ will yield solutions of the form μ/σ = k (k being a constant). That is, μ linearly scales with σ, and the slope of this relationship, k, is given by solving (5) for μ/σ. As (5) is a rather challenging algebraic equation to solve for μ/σ, we used an analytic solver (Matlab's Symbolic Math Toolbox). A plot of the relationship between μ and σ that we found using the solver is shown in Figure S8A using the lag-1 values for C_p and C_n estimated from our data. Note that μ monotonically increases with σ, but that this increase is rather small in amplitude in line with our intuition that the small carryover gains and the small asymmetry between carryover gains that we find would lead to only minor increases in μ as σ increases. Note also that σ in the equations above refers to variability in GF production, rather than environmental variability. While it is true that increases in environmental variability should lead to increases in the variability of GF production, these two quantities are only indirectly related. Thus to obtain an estimate of the relationship between carryover-driven effects on μ and the environmental variability that was controlled in our experiments, we combined (a) the relationship between μ and output variability solved for above and (b) the relationship between output variability and environmental variability observed in our data. The result gives the apparent sensitivity of GF levels to changes in environmental variability that could come from the slightly asymmetric trial-to-trial carryover effects we observe.

We repeated the above procedure for different ranges of lags (values of N in Equation 1) of up to 50 movements, each of which leads to a different value for C_p and for C_n, derived from the carryover gains we observe at different lags. We found that, when only next-movement carryover effects are taken into account, the effect is nearly zero, amounting to an apparent sensitivity of GF against environmental variability equal to 0.009 (see the first point in Figure S8B). If we instead consider the combined effect of all 50 carryover gains shown in Figure S7E,F we also find an effect that is essentially zero in amplitude, amounting to an apparent sensitivity of GF against environmental variability equal to -0.02 (see the 50th point in Figure S8B). However, since we don't a priori know how many carryover gains should be considered, we made the above sensitivity calculation for all intermediate lag ranges (each extending from a lag of 1 to a lag between 1 and 50). The results for this series of calculations are shown in Figure S8B. Note the values we found using lag ranges extending to 10 or 20 trials were somewhat higher than that what we observed below 10 or above 20, but that all values here are small with gains of less than 0.1.

To double check this calculation, we validated the preceding analysis by simulating Equation 1 and obtaining estimates of the effect of asymmetric carryover effects on the apparent sensitivity of GF levels. This gave similar results (green trace in Figure S8B) to the analytic solution described above (orange trace). Thus, the relatively small carryover we observe (all carryover gains less than 0.17) and the even smaller carryover asymmetries (asymmetries were not exclusively positive, and the maximum positive asymmetry was less than 0.06) appear to result in little effect for the sensitivity of GF to environmental variability.

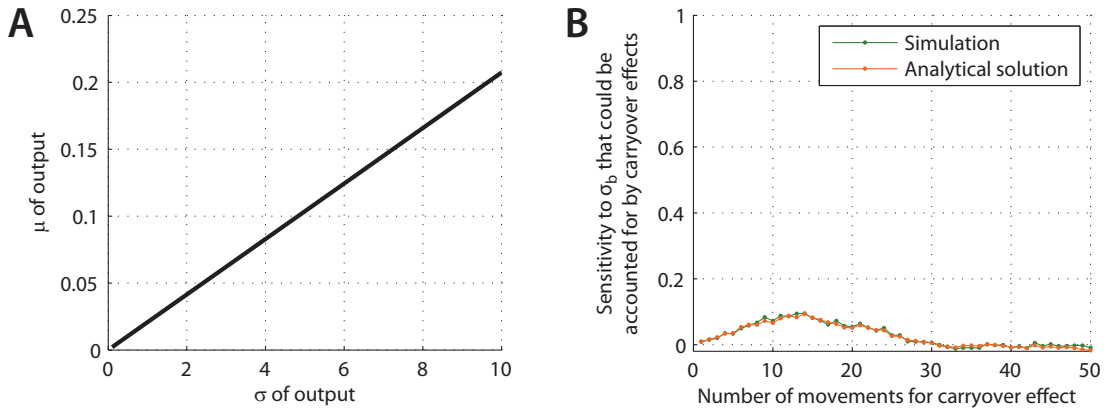

Figure S8: Modeling the effects of the small asymmetries in carryover shows that any effects are minimal.

A: The relationship between the mean, μ, and the standard deviation, σ of the output based on Equation (4), showing a strongly linear relationship between the two. B: Shown is the expected contribution of carryover effects onto the apparent sensitivity of GF against environmental variability (green: simulation; orange: based on the analytical solution of equation (4)) against increasing ranges of carryover lags taken into account (x-axis). Note that the effect of carryover does not result in sensitivities larger than about 0.10 in any case; That is 10% or less of the GF sensitivity to environmental variability that we observe (which is equal to 1.00 ±0.10 based on Experiments 1a, 1b, and 1c together).

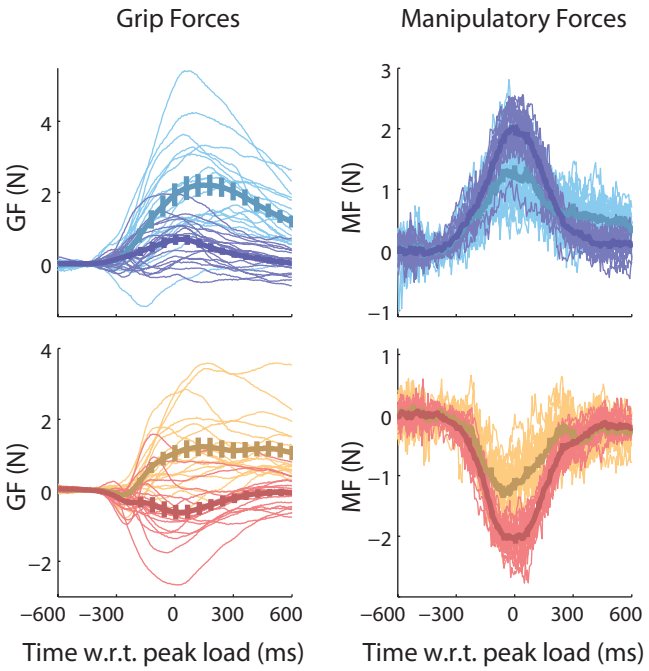

Figure S9. The individual grip and manipulatory force profiles early and late in Experiment 2 are characteristic of subject-average behavior. Thin lines indicate data from individual subjects; thick lines indicate across-subject mean±SEM.

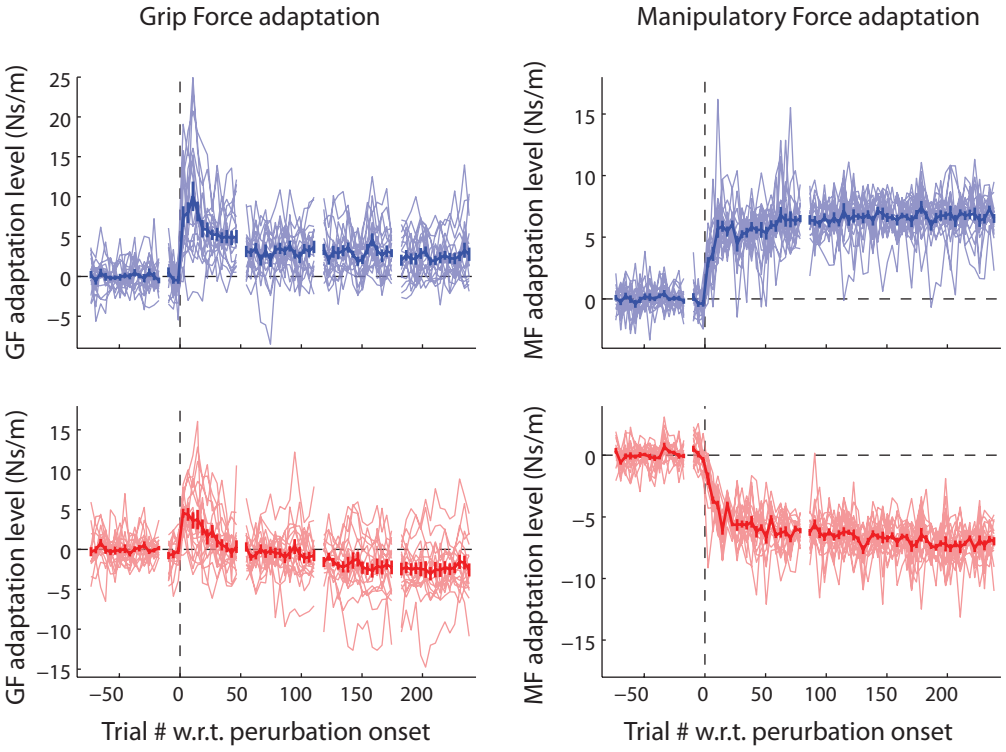

Figure S10. Individual adaptation curves for grip and manipulatory forces in Experiment 2. Thick lines indicate subject average ± SEM, whereas thin lines indicate individual subject data. Blue: +FF; red: -FF. Note how most subjects follow the same GF adaptation pattern: overshoot during early +FF adaptation, and inappropriate (>0) responses during early –FF adaptation.

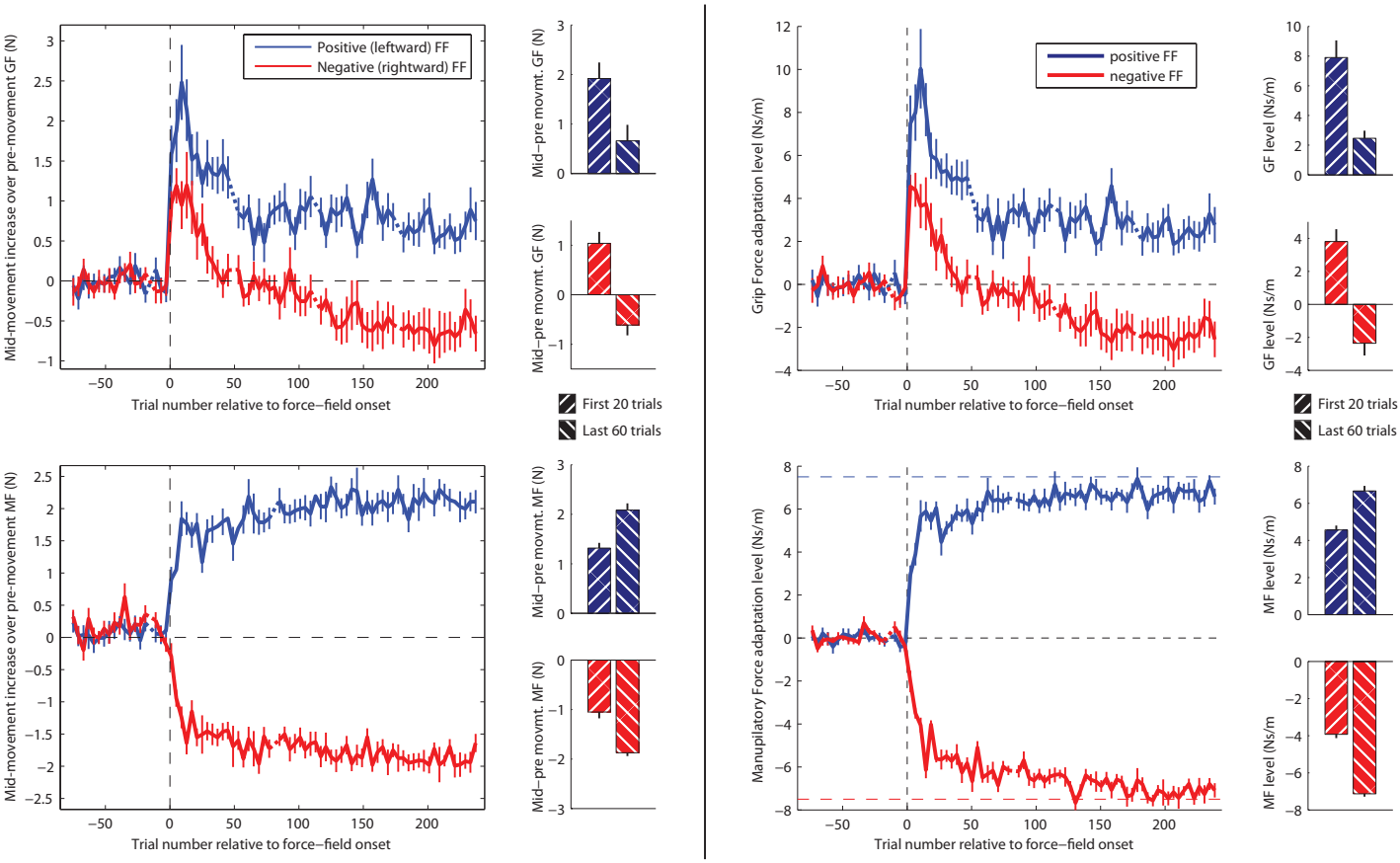

Figure S11. Results from Experiment 2 are robust under different metrics.
Learning curves for GF and MF in experiment 2. Analogous to Figure 5 panels C-E & H-J (reproduced to the right) but adaptation levels were calculated based on the difference between the mid-movement (peak speed) force level and the pre-movement force level (100 to 250ms before movement onset). Note how the shape of the adaptation curves for both GF and MF is very similar with Figure 5 (which used a linear regression measure), in spite of the different range and different units between these two metrics.

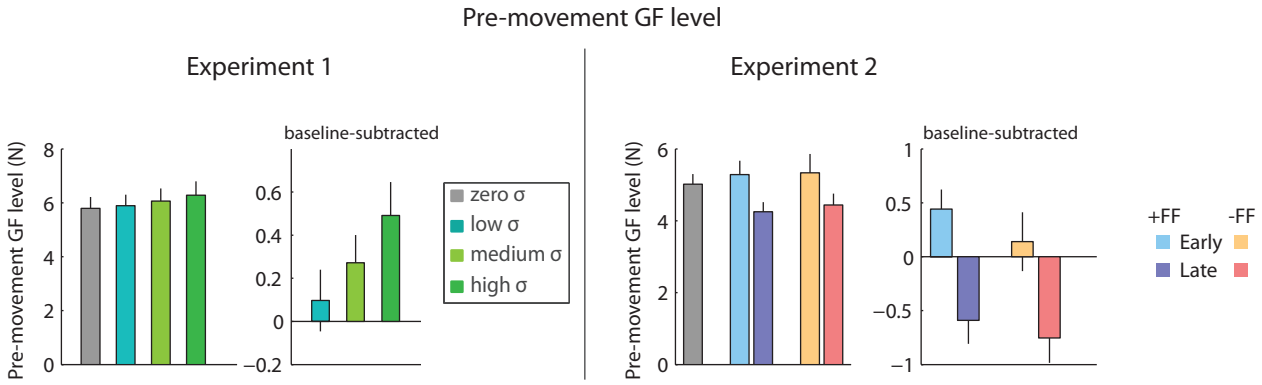

Figure S12. Pre-movement grip forces for the different variability levels in Experiment 1 (left) and for early vs. late adaptation in Expt 2. Note that pre-movement GFs are higher when variability is increased (medium- and high-σ blocks in Expt 1, but also early adaptation in Expt 2).